INDERSCIENCE PUBLISHERS
Linking academia, business and industry through research

International Journal of Quality Engineering and Technology

ISSN online: 1757-2185 - ISSN print: 1757-2177
https://www.inderscience.com/ijqet

A new rotating machinery fault diagnosis method based on data driven and expert knowledge

Zhenghui Li, Na Zhang, Feiya Lv, Jingya Yang, Rui Wang

DOI: 10.1504/IJQET.2023.10060526

Article History:

Received:	10 June 2022
Last revised:	15 February 2023
Accepted:	29 April 2023
Published online:	25 July 2024

A new rotating machinery fault diagnosis method based on data driven and expert knowledge

Zhenghui Li* and Na Zhang

Henan Engineering Research Center of
Rail Transit Intelligent Security,
461200, Zhengzhou, Henan, China
Email: 15858190140@163.com
Email: 1453698002@qq.com
*Corresponding author

Feiya Lv

School of Software,
Anyang Normal University,
455002, Anyang, China
Email: Lvfeiya0215@126.com

Jingya Yang and Rui Wang

Henan Engineering Research Center of
Rail Transit Intelligent Security,
461200, Zhengzhou, Henan, China
Email: yang_jing_ya@126.com
Email: 664068648@qq.com

Abstract: This paper presents data driven and expert knowledge method for diagnosing rotating machinery fault. The belief rule-based (BRB) inference method is used to model the complex nonlinear relationship between the abnormal vibration features of rotating machinery and its fault type. If the data of all features are used for diagnosis, then computation burden will be too large to realise real-time diagnosis. First, the inputs of BRB model are reduced and weighted through neural network based on data driven algorithm. The outputs of BRB model are fault types of rotating machinery. The belief rules activated by the inputs are combined by the evidential reasoning (ER) algorithm so as to obtain the fused belief structure about the fault, and then, the accurate diagnose result can be calculated from the fused result. The diagnosis results cannot only judge the fault type, but also give the probability of potential fault. The model parameters are open and interpretable. Finally, in the experiment of fault diagnosis of motor rotor, the effectiveness of the proposed method is illustrated.

Keywords: fault diagnosis; rotating machinery; data driven; expert knowledge.

Reference to this paper should be made as follows: Li, Z., Zhang, N., Lv, F., Yang, J. and Wang, R. (2024) 'A new rotating machinery fault diagnosis method based on data driven and expert knowledge', *Int. J. Quality Engineering and Technology*, Vol. 10, No. 1, pp.1–18.

Biographical notes: Zhenghui Li is currently an Associate Professor with Henan Engineering Research Center of Rail Transit Intelligent Security, Zhengzhou Railway Vocational & Technical College, Zhengzhou, China. His current research interests include artificial intelligence, fuzzy set theory, Dempster-Shafer evidence theory and its applications in the processing of uncertain information, condition monitoring, safety evaluation, and fault diagnosis of complex industrial systems.

Na Zhang is currently a Lecturer with Henan Engineering Research Center of Rail Transit Intelligent Security, Zhengzhou Railway Vocational and Technical College, Zhengzhou, China. His current research interests include state estimation, fault detection, belief rule base reasoning and its applications in complex industrial systems, and the processing of uncertain information.

Feiya Lv received her PhD in Control Science and Engineering from Zhejiang University, Hangzhou, China in 2019. She was with the Institute of Anyang Normal University, Anyang, Henan, China. Her current research interests include robust control, neural network, networked control system, fault diagnosis, and fault-tolerant control.

Jingya Yang received her PhD degree in Beijing Jiaotong University, Beijing, China in 2019. She is currently an Associate Professor with the Institute of Henan Engineering Research Center of Rail Transit Intelligent Security, Zhengzhou Railway Vocational and Technical College, Zhengzhou, China. Her current research interests include multisource network information fusion theory and method, multi-target tracking theory, and complex industrial systems/fault detection.

Rui Wang is currently a Lecturer with Henan Engineering Research Center of Rail Transit Intelligent Security, Zhengzhou Railway Vocational and Technical College, Zhengzhou, China. His current research interests include intelligent information processing and Dempster-Shafer evidence theory.

1 Introduction

Rotating machinery is the key equipment in power, petrochemical, metallurgy and other pillar industries of national production, as shown in Figure 1. With the increase of running speed, load and automation of rotating machinery equipment, and the actual demand for long-term continuous operation in complex industrial environment, once the fault or any damage occurs in the equipment, which will directly affect its normal operation in industrial applications, resulting in serious accidents and economic losses (Sun et al., 2013; Xu et al., 2017). Therefore, in order to ensure the continuous, stable and safe operation of rotating machinery in industrial application, it is necessary and meaningful to diagnose accurately the rotating machinery fault (Gonza et al., 2020; Choudhary et al., 2020). The importance of rotating machinery fault diagnosis comes from the serious need for continuous monitoring of the health of the industrial components and systems through their life (Omar et al., 2021; Musaw et al., 2020).

The essence of rotating machinery fault diagnosis is to identify the abnormal working conditions of rotor system, gearbox and other components (Yu et al., 2020; Chen et al., 2020). There are many researches on fault diagnosis of rotating machinery in recent

years, which are mainly divided into four categories: fault diagnosis based on analytical model, fault diagnosis based on signal/image processing, fault diagnosis based on data-driven and fault diagnosis based on expert knowledge (Gao et al., 2015; Omar et al., 2020; Devarajan et al., 2021; Choudhary et al., 2021). Analytical model-based fault diagnosis method has the advantage of penetrating into the essence of object and real-time fault diagnosis, and fault characteristics of system are usually closely related to model parameters, such as turbine motor fault diagnosis (Alhelou et al., 2018). However, for complex rotating mechanical systems, the cost of establishing analytical model is too high to affect its wide application in this field. Signal/image processing-based fault diagnosis method mainly analyse various sensor information to diagnose equipment fault types (Yan et al., 2020; Atamuradov et al., 2020). Thermographic fault diagnosis of ventilation in BLDC (brushless DC) motors is described (Glowacz, 2021). The main disadvantages of this method are as follows:

1 expensive sensor is required

2 It cannot be used as early fault detection and diagnosis (Omar et al., 2020).

Sounds and acoustic emission principle is used for early fault diagnosis of induction motor (Omar et al., 2021; Pham et al., 2020). This method has the ability of easy implementation, fault location and high frequency processing. But at the same time, this method is too sensitive to noise and requires expensive sensors (Omar et al., 2020). Because vibration information has unique advantages in characterising the fault state of rotating machinery, it is an effective method to diagnose the fault of rotating machinery, such as the early fault diagnosis method of rotating machinery based on empirical mode (Gao et al., 2021; Wu et al., 2016). However, in the noise environment of complex mechanical system, vibration information often has the characteristics of strong uncertainty and randomness. Most of the existing methods use single source information for fault diagnosis, which is easy to cause mis-judgment and uncertainty of diagnosis results. The data-driven fault diagnosis method can distinguish the normal mode and fault mode of the system by obtaining the hidden deep-seated feature information. This method uses the collected monitoring data and various data mining technologies to obtain the above hidden feature information. Artificial Intelligence method is one of the data-driven methods, such as support vector machine and deep neural network (Wu et al., 2020; He and He, 2020). Because of its strong fault feature extraction ability, it has been widely applied in the field of fault diagnosis (Wang et al., 2021; Wu et al., 2019), but the training of classification model often requires a large amount of sample data, otherwise the model is prone to over fitting. In order to increase diagnostic performance, knowledge-based intelligent systems should be further investigated (Omar et al., 2020; Bui et al., 2020). The fault diagnosis method based on expert knowledge uses incomplete prior knowledge to describe the functional structure of the system, and predicts the system fault according to the established qualitative reasoning model. Because it is difficult to determine the accurate model of rotating machinery, this method has attracted more and more scholars' attention (Alhelou et al., 2018; Cheng et al., 2022).

In view of the above problems, this paper proposes a novel rotating machinery fault diagnosis method based on data-driven and expert knowledge. This method ingeniously fuses the fault feature mining ability of data-driven method and the advantages of expert knowledge method in dealing with uncertain information. Aiming at the random interference of a single information source in space, a multi-source vibration information

sensing mechanism is designed. However, if the data of all features are used for diagnosis, then computation burden will be too large to realise real-time diagnosis. The data-driven neural network method is used to extract important fault feature information as model input. The BRB is used to model the complex non-linear relationship between the abnormal vibration features of rotating machinery and its fault type. The belief rules activated by the inputs are combined by the evidential reasoning (ER) algorithm (Zhou et al., 2019; Song et al., 2022) so as to obtain the fused belief structure about the fault, and then, the accurate diagnose result can be calculated from the fused result. The diagnosis results cannot only judge the fault type, but also give the probability of potential fault. The model parameters are open and interpretable.

Figure 1 Application of rotating mechanical equipment in various fields (see online version for colours)

2 Problem description and belief rule base theory

2.1 Problem description

In practical engineering applications, rotating machinery often runs under heavy load, long-time operation and other harsh conditions. This above working conditions will easily lead to rotor unbalance, rotor misalignment, pedestal looseness, connector looseness, gear tooth missing and other faults in rotating machinery. These faults often lead to varying degrees of nonlinear vibration of rotating machinery (Wu et al., 2019). If the fault diagnosis model is constructed by nonlinear vibration data, the fault type and degree of rotating machinery can be diagnosed timely and accurately. It is helpful to improve the level of status maintenance and realise the health life cycle management of rotating machinery. The advantage of this method is the fault diagnosis model based on monitoring vibration data and expert knowledge, which can judge the health state of rotating machinery without shutdown maintenance, so as to adjust the maintenance cycle and ensure the stable and safe operation of rotating machinery.

There are two main problems to be solved in this paper:

Problem 1: How to use the monitoring vibration data and expert knowledge to establish the fault diagnosis model of rotating machinery based on the belief rule base reasoning. Therefore, the fault diagnosis model is established as follows:

$$F_i = f\left(x_1, x_2, \cdots, x_T, R\right), \tag{1}$$

where *Fi* represents the fault type of rotating machinery, *x* represents the fault features information, *f*(•) represents the nonlinear mapping function and *R* represents the expert knowledge.

Problem 2: If the input information of BRB is too much, the number of combination rule will increase explosively, which seriously affects the real-time performance of fault diagnosis. However, at the same time, the fault feature information is too little to represent the fault type. Therefore, the MIV algorithm is used to pick out the fault characteristic factors which are highly correlated with the fault features, and then the fault characteristic factors are used to model and diagnose the fault, which will improve the diagnosis rate and real-time performance of the model. The filtering model is established as follows:

$$Q\left(c_i, \delta_i\right) = q\left(c_1, c_2, \cdots, c_n, F\right), \tag{2}$$

where $Q(c_i, \delta i)$ is the reduced and weighted information, δ is the attribute weight, $q(c_1, c_2, \ldots, c_n, F)$ is the input information, *c* represents the reduced and weighted feature information, and *F* represents the fault type.

2.2 Belief rule base theory

In the actual high-noise working environment of rotating machinery, there is a strong nonlinear characteristic between fault feature and type. At the same time, the vibration sensor used to collect fault feature information has its own systematic error. These factors greatly increase the uncertainty of fault diagnosis model. The belief rule base reasoning method cannot only integrate subjective and objective information, but also use ER process to reason uncertain information, which has unique advantages of uncertain nonlinear modelling. Moreover, the physical meaning of model parameters is interpretable, so it has friendly practical value. The belief rule base is composed of a series of belief rules with the same structure, and the belief structure in the evidence form is used to describe the latter attribute of the belief rule. The belief rule is expressed as (Li et al., 2017):

R_k: If $x_1 = A_1^k$ and $x_2 = A_2^k$ and $x_3 = A_3^k$, then $\{(F_6, \beta_{6,k}), (F_5, \beta_{5,k}), \ldots, (F_1, \beta_{1,k})\}$ with rule weights θ_k, attribute weights δ_1, δ_2, δ_3, where *k* represents the k^{th} belief rule, x_1, x_2, x_3 represents the amplitude change of 1X~3X frequency doubling, A_1^k, A_2^k, A_3^k respectively represent the reference value of the input attribute. $x_1 = A_1^k$ and $x_2 = A_2^k$ and $x_3 = A_3^k$ constitute the antecedent of the belief rule, F_1, F_2, …, F_6 represent the six fault types, $\beta_{j,k}$ represents the belief degree to each fault type, and *j* represents the j^{th} fault type, those together constitute consequent of the belief rule. When $\beta_{j,k} = 1$, the consequent of the belief rule is $(F_j, 1)$, the belief rule is degenerated to a general IF-THEN form.

3 Rotating machinery fault diagnosis model based on data driven and expert knowledge

This fault diagnosis model is mainly divided into three parts:

1 Fault feature extraction based on data driven method.

2 Reasoning process of fault diagnosis model.

3 Model optimisation.

The detailed steps of fault diagnosis model are described in the block diagram, as shown in Figure 2.

3.1 Fault feature extraction based on data driven method

The mean impact value (MIV) is based on BP neural network, which represents the importance weight of each variable affecting the dependent variable. If there is a small change $\Delta\omega_{ij}$ of the connection weight between the input layer and the hidden layer, this change will be passed to the output S_j of the hidden layer and make it change Δs_j, and then the change e_k of the network output will be generated. The weight ω_{ij} and ω_{ik} will be updated through the reverse transfer. The loss function is defined as follows (Ji et al., 2017):

$$E(e)=\frac{1}{2}\sum_{j=1}^{n}e_k^2=\frac{1}{2}\sum_{j=1}^{n}\left[\hat{y}(k)-y(k)\right]^2. \tag{3}$$

For the fault feature dataset X = [x(1), x(2) … x(L)], self-increase and self-decrease operations are carried out for a feature variable in each sample data.

$$X_{\pm\delta}^{(i)}=\left[x_{\pm\delta}^{(i)}(1),x_{\pm\delta}^{(i)}(2),\cdots,x_{\pm\delta}^{(i)}(L)\right], \tag{4}$$

$$x_{\pm\delta}^{(i)}(w)=\left[x_1(w),\cdots,(1\pm\delta)x_i(w),\cdots,x_n(w)\right]^T, \tag{5}$$

where L represents the number of fault feature factors and n represents the number of sample groups. The fitting output of the neural network is shown as follows:

$$\hat{Y}_{i,\pm}=\sum_{k=1}^{L}Z_j\omega_{jk}+b_k, \tag{6}$$

$$Z_j=f\left(\sum_{i=1}^{n}\omega_{ij}x_{\pm\delta}^{(i)}(w)+a_j\right). \tag{7}$$

If $\hat{Y}(w)=F\left(x_1(w),x_2(w),\cdots,x_n(w)\right.$, then

$$\begin{aligned}IV_i&=\hat{Y}_{i,+}-\hat{Y}_{i,-}\\&=F\left(x_1(w),\cdots,(1+\delta)x_i(w),\cdots,x_n(w)\right)\\&\quad -F\left(x_1(w),\cdots,(1-\delta)x_i(w),\cdots,x_n(w)\right).\end{aligned} \tag{8}$$

So, $0.1 \le \delta \le 0.3$, $i = 1, 2, \ldots, n$. $\hat{Y}_{i,+}$ and $\hat{Y}_{i,-}$ respectively represent the network output results of sample set $X_{\delta_i^+}$ and $X_{\delta_i^-}$. The impact value of each fault feature variable on the fault type in the sample is expressed as:

$$IV = [IV_1, IV_2, \cdots, IV_n]^T, \tag{9}$$

Then, taking the average value of IV according to the number of observed column, the MIV of fault feature on the final output fault type can be calculated as:

$$MIV = \frac{1}{L}\sum_{i=1}^{L} IV_i. \tag{10}$$

3.2 Reasoning process of fault diagnosis model

According to the MIV of fault feature and expert knowledge, reduced fault feature c and weighted attribute weight are used to construct the initial belief rule base. The rule in the belief rule base will be activated to varying degrees by input fault feature data. The activation weight wk can be defined as

$$w_k = \theta_k \prod_{i=1}^{M} \left(\alpha_i^k\right)^{\bar{\delta}_i} \Bigg/ \sum_{k=1}^{T} \left[\theta_k \prod_{i=1}^{M} \left(\alpha_i^k\right)^{\bar{\delta}_i} \right], \tag{11}$$

where $\bar{\delta i}$ is the relative attribute weight of the activated rule

$$\bar{\delta}_i = \delta_i \Big/ \max_{i=1,2,\ldots H} \{\delta_i\}. \tag{12}$$

There is a certain matching degree α_i^k between the input variable x_i and the antecedent reference value A_i^k, $A_i^k \in \left\{A_{i,1}^k, A_{i,2}^k, ..., A_{i,H}^k\right\}$; If x_i is less than or equal to the minimum in A_i^k, or greater than or equal to the maximum in A_i^k, the matching degree α_i^k between x_i and A_i^k is 0 or 1. Otherwise, the matching degree α_i^k can be expressed as

$$\alpha_{i,q}^k = \left(A_{i,q}^k - x_i\right) / \left(A_{i,q+1}^k - A_{i,q}^k\right), \tag{13}$$

$$\alpha_{i,q+1}^k = \left(x_i - A_{i,q}^k\right) \Big/ \left(A_{i,q+1}^k - A_{i,q}^k\right). \tag{14}$$

The belief rules activated at varying degree are discounted according to w_k and α_i^k, and then the consequent structure of the discounted belief rule can be fused by evidence reasoning theory. The fusion result can be calculated as

$$O(X) = \left\{\left(F_j, \beta_j\right), j = 1, 2, \cdots, 6\right\}, \tag{15}$$

which

$$\beta_j = \frac{u\left[\prod_{k=1}^{T}\left(w_k\beta_{j,k}+1-w_k\sum_{i=1}^{N}\beta_{i,k}\right)-\prod_{k=1}^{T}\left(1-w_k\sum_{i=1}^{N}\beta_{i,k}\right)\right]}{1-u\left[\prod_{k=1}^{T}(1-w_k)\right]}, \tag{16}$$

$$u = \left[\sum_{j=1}^{N}\prod_{k=1}^{T}\left(w_k\beta_{j,k}+1-w_k\sum_{i=1}^{N}\beta_{j,k}\right)-(N-1)\prod_{k=1}^{T}\left(1-w_k\sum_{i=1}^{N}\beta_{i,k}\right)\right]^{-1}. \tag{17}$$

Figure 2 The block diagram of fault diagnosis model

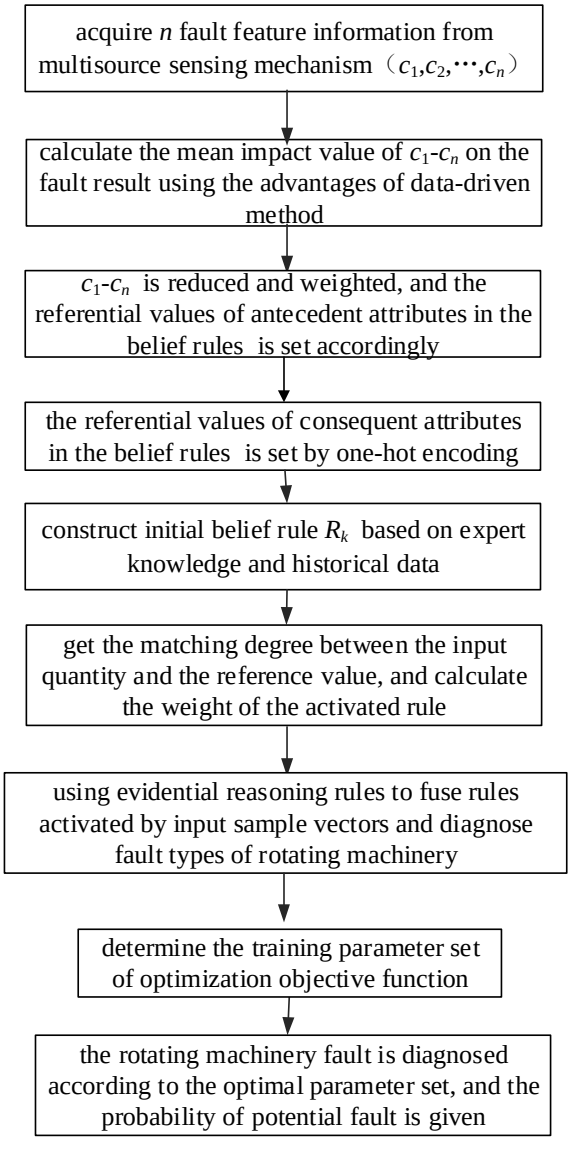

From (15), $\sum_{j=1}^{6}\beta_j = 1\left(0 \le \beta_j \le 1\right)$, β_j represents the support degree of fusion result to fault type F_j. If MAX(β_1, β_2, …, β_j, …β_6) = β_j, which means that the probability of rotating machinery fault F_j is the highest, and the diagnosis result is $\hat{F} = F_j$.

3.3 Model optimisation

Because of the complex internal mechanism of rotating machinery equipment, it is difficult for experts to determine the exact values of all parameters in the fault diagnosis model. Therefore, it is necessary to fine-tune the initial parameters to improve the accuracy of the model. However, the fusion result of the confidence rule base is the probability of various fault types, which cannot be directly used to calculate the deviation between the diagnosis result and the real value. Therefore, the fault types are coded as one-hot encoding, which extends the discrete attribute features to Euclidean space. The fault coding of rotating machinery is shown in Table 1.

The Euclidean distance between the system output and the actual output is taken as the objective function of parameter optimisation:

$$f(P) = \left\{\frac{1}{l}\sum_{t=1}^{l}\left[\left\|Ture\_F(t) - Estimated\_F(t)\right\|^2\right]^2\right\}^{\wedge 0.5}. \tag{18}$$

From (18), *Estimated_F*(*t*) is the output diagnosis result of the t^{th} group input data. *Ture_F*(*t*) is the one-hot encoding of the actual fault type of the t^{th} group input data. l represents the group number of sample data; P represents the optimisation parameters set (rule weight θ_k, consequent confidence $\beta_{j,k}$, attribute weight δ_k), and the constraint condition is $0 \le \theta_k \le 1, 0 \le \delta_k \le 1, 0 \le \beta_{j,k} \le 1$ $\sum_{j=1}^{6}\beta_{j,k} = 1$.

Table 1 Fault type and code

Number	*Fault types*	*Code*
F6	Normal operation	100000
F5	Rotor unbalance	010000
F4	Rotor misalignment	001000
F3	Pedestal looseness	000100
F2	Connector looseness	000010
F1	Gear tooth missing	000001

4 Experimental test

4.1 Problem description

In this paper, a basic motor rotor in rotating machinery is taken as an example to verify the effectiveness of the proposed method by using ZHS-2 multi-functional motor flexible rotor system. In different directions of the rotor support part of the experimental platform,

size frequency-domain vibration acceleration sensors are installed to sense the fault state of the motor rotor. In order to avoid mutual interference of multiple sensors in space, we only install 1–2 sensors at a time to collect vibration data, as shown in Figure 3. Figure 3 shows two acceleration vibration sensors installed in the horizontal and vertical directions of the support frame. The other three acceleration vibration sensors are installed in different directions on the motor bracket in turn. Because different motor rotor fault types will cause the vibration amplitude variation of multi-frequency components, the amplitude variation in the frequency domain of 1X~3X multiple frequency is obtained as the model input. When the motor speed is set to 1,500 r/m, then the fundamental frequency 1 X is 25 Hz, and the n multiple frequency $nX(n = 1, 2, 3, \ldots)$ is $(n \times 25)$ Hz. For each rotor fault type, 15 fault features (c_1, c_2, …, c_{15}) of 1X~3X multiple frequency are obtained from five vibration sensors , and 210 sets of sample data are collected in experimental test (100 sets of data are used for model training, 110 sets of data are used for model testing).

Figure 3 Experimental platform of motor rotor system

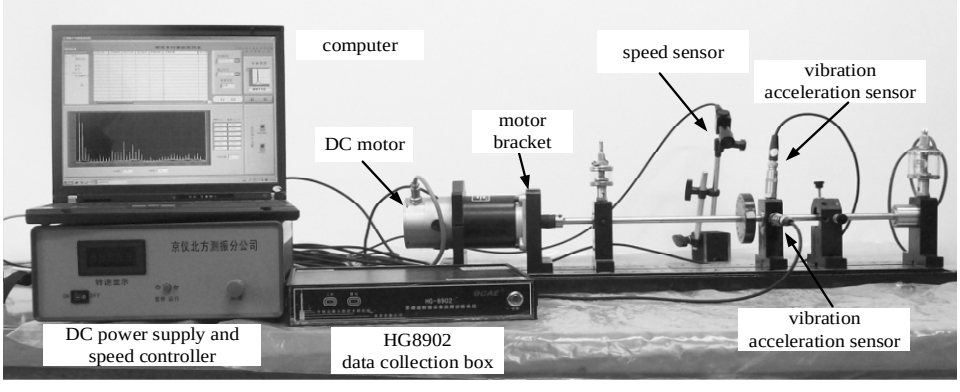

4.2 Reduced weighted feature based on MIV

The simulation results are obtained under the following simulation conditions: the maximum iteration number of the network is set to 2,000, the minimum target error is $1.0*e^{-5}$, and the increment is 0.1. Based on the trained BP neural network, the mean influence value of c_1–c_{15} fault features are calculated by MIV algorithm. According to the above MIV of fault features, the high sensitive region of fault features can be obtained, which means that the selected fault features can better characterise the fault diagnosis information. The high sensitive region is shown in Figure 4.

The fault feature c_3, c_5 and c_{13} are selected as the high impact factor in the high sensitive region, and their MIV is calculated as 1.1143, 0.6876 and 0.4902 respectively. Then from equation (7), the relative weights of the selected fault features are obtained as 0.4057, 0.2504 and 0.1785.

Figure 4 The MIV of the fault feature c_1–c_{15}

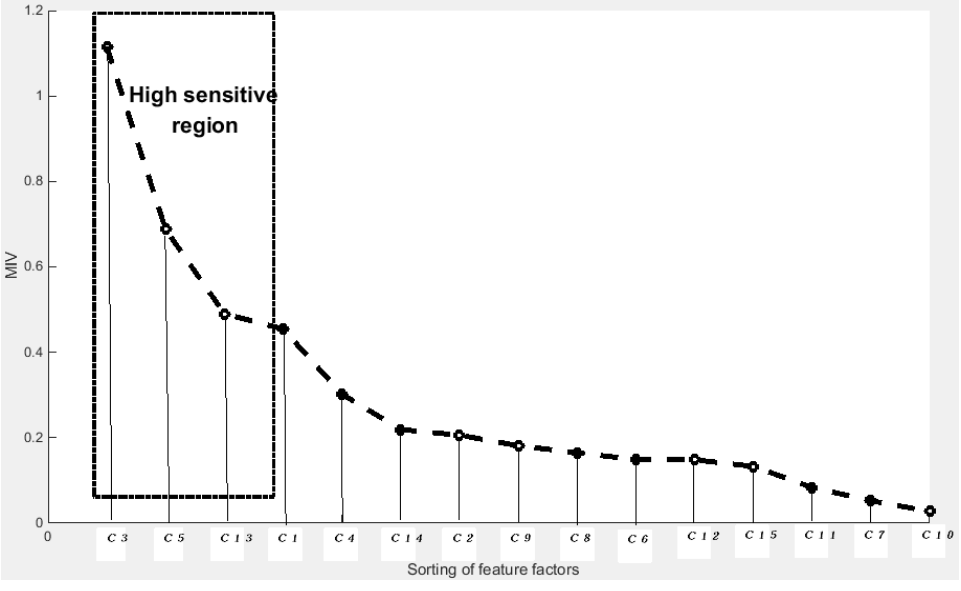

Figure 5 The corresponding trend between c_3, c_5, c_{13} and 6 fault types (see online version for colours)

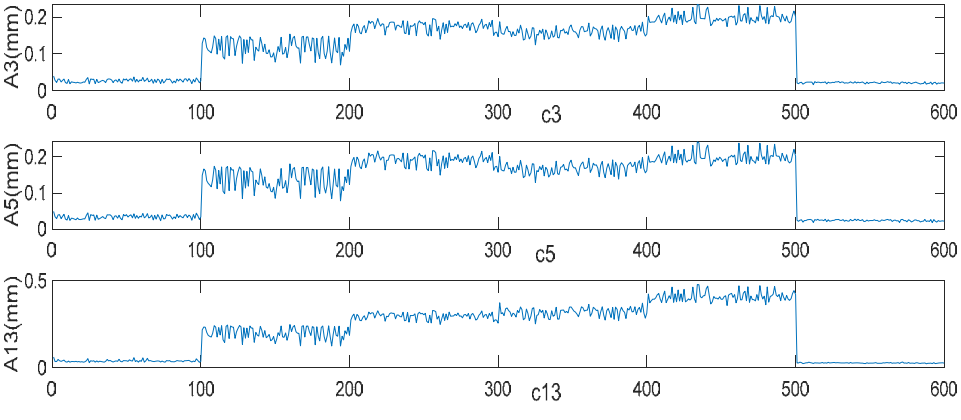

4.3 Construction of initial belief rule base

The 600 sets sample data of the selected fault feature c_3, c_5 and c_{13} are collected by motor flexible rotor system. The nonlinear relationship between the selected fault features and fault diagnosis types is shown in Figure 5. It is obvious that the fault features selected by the MIV algorithm can more accurately characterise the occurrence trend of six fault types.

Our primary mission is to set the referential values of antecedent and consequent attributes in the belief rules. According to the sample information of fault feature data, we set 5 antecedent referential value for c_3, c_5, c_{13}, namely, positive very small (VS), positive

small (PS), positive medium (PM), positive large (PL) and positive very large (VL) with their values as follows:

- A_1^k {0.0942(VS), 0.1187 (PS), 0.1851 (PM), 0.1959(ML), 0.2051(VL)}.
- A_2^k {0.0776(VS), 0.0861(PS), 0.1717 (PM), 0.1814(ML), 0.2062(VL)}.
- A_3^k {0.0715(VS), 0.0806 (PS), 0.1338 (PM),0.1859(ML), 0.2262 (VL)}.

For the consequent attribute of the fault diagnosis type, one-hot encoding is used to describe the consequent attribute. The belief rules can be expressed as R_k: if $X_1 = A_1^k$ and $X_2 = A_2^k$ and $X_3 = A_3^k$, then Y is {(D_1, $\beta_{k,1}$)... ,(D_N, β_k, N)}, where $N = 6$, $\sum_{j=1}^{N} \beta_{j,k} = 1$, $k = 1, 2..., 125$. The initial value of weight θ_k for each rule is set to 1, and the initial value of attribute weight is set to $\delta_1 = 0.4057$, $\delta_2 = 0.2504$, $\delta_3 = 0.1758$ in Section 4.2. Table 2 lists the partial rules in the initial BRB.

After the initial BRB is constructed based on expert knowledge and historical data, the detailed fault diagnosis process is as follows:

Step 1 Calculate the matching degree of the input

The 600 sets sample data of fault feature c_3, c_5 and c_{13} are taken as BRB input, and the matching degree of each set sample data for A_1^k, A_2^k and A_3^k is calculated by equations (13) and (14). For example, when the 118th set of fault feature data is input, and the input variable is X = [0.0776, 0.0855, 0.1380], then the matching degree of X_1(0.0776) to reference point (PS, PM) are calculated as 0.4478 and 0.5522, and the matching degree of X_2(0.0855) to reference point (PM, ML) are calculated as 0.8773 and 0.1227, and the matching degree of X_3(0.1380) to reference point (PS, PM) are calculated as 0.5585 and 0.4415, and the matching degree for other reference points is 0.

The 600 sets sample data of fault feature c_3, c_5 and c_{13} are taken as BRB input, and the matching degree of each set sample data for A_1^k, A_2^k and A_3^k is calculated by equations (13) and (14). For example when the 118th set of fault feature data is input, and the input variable is X = [0.0776, 0.0855, 0.1380], then the matching degree of X_1(0.0776) to reference point (PS, PM) are calculated as 0.4478 and 0.5522, and the matching degree of X_2(0.0855) to reference point (PM, ML) are calculated as 0.8773 and 0.1227, and the matching degree of X_3(0.1380) to reference point (PS, PM) are calculated as 0.5585 and 0.4415, and the matching degree for other reference points is 0.

Table 2 Partial rules in the initial BRB

No	θ_k	*X_1 and X_2 and X_3*	*Y*					
			β_1	β_2	β_3	β_4	β_5	β_6
1	1.0	VS and VS and VS	0	0	0	0	0.02	0.98
25	1.0	VS and VL and ML	0	0	0	0.28	0.72	0
50	1.0	PM and VL and VS	0	0	0.25	0.75	0	0
100	1.0	PM and PS and VL	0	0	0.89	0.11	0	0
125	1.0	VL and VL and VL	0.68	0.32	0	0	0	0

Step 2 Calculates the weight of the activated belief rule

After the matching degree α_i^k of the input to the reference point in each rule is obtained, these matching degrees are substituted into equations (11) and (12) to get the activation weights for total 125 rules in Table 2 in which eight rules are activated with No = 37, 38, 42, 43, 62, 63, 67, 68. The corresponding weights are w_{37} = 0.2195, w_{38} = 0.1734, w_{42} = 0.0307, w_{43} = 0.0243, w_{62} = 0.2706, w_{63} = 0.2139, w_{67} = 0.0378, w_{68} = 0.0299 respectively. That is to say, the activation weights of other rules are all 0.

Step 3 Fuse those activated belief rule base on evidence reasoning

The above activated rules are fused by evidence reasoning method, and the structure of the fused consequent is

$$O(X) = \left\{ \left(F_j, \beta_j \right), j = 1, 2, \cdots, 6 \right\}$$

where, F_j and β_j can be calculated by equations (16) and (17) respectively. For example, the w_k and $\beta_{j,k}$ of the 118th set fault feature data are substituted into equation (15) to get $O(X)$ = {(F_1, 0), (F_2, 0), (F_3, 0), (F_4, 0.0073), (F_5, 0.7968), (F_6, 0.1959)}.

Step 4 Diagnosis fault result of the motor rotor

According to the above fusion result in step3, the fault type corresponding to the maximum belief degree value is the diagnosis fault result. For example, for the 118th set fault feature data, the corresponding fault diagnosis result is rotor unbalance (β_5 = 0.7968), and the potential fault type is normal operation (β_6 = 0.1959). Finally, the Euclidean distance error (Δ = 0.2032) based on the one-hot encoding is calculated by equation (18).

Table 3 The diagnosis results of the initial belief rule base

		Fault diagnosis result							
		F6	*F5*	*F4*	*F3*	*F2*	*F1*	*Total*	*Diagnostic accuracy*
Fault type	F6	78	8	3	0	0	11	100	78%
	F5	10	88	2	0	0	0	100	88%
	F4	0	6	80	8	6	0	100	80%
	F3	0	0	5	91	4	0	100	91%
	F2	0	0	0	5	86	9	100	86%
	F1	10	0	0	3	7	80	100	80%

600 sets of c_3, c_5 and c_{13} data samples are input into the initial belief rule base, and the diagnosis results are shown in Table 3. The diagnostic accuracy of the proposed method for six fault types is 78%, 88%, 80%, 91%, 86% and 80% respectively, and the overall diagnostic accuracy is 83.83%. At the same time, in order to verify the discrete degree of this method, 50 sets of sample data are randomly selected as one group, a total of 12 groups. The root mean square error (RMSE) between the diagnosis results of 12 groups data and the real fault type is calculated as 0.4572. The results show that the discrete

degree of the method is smaller, the belief of the diagnosis is more concentrated, and the fault features selected by MIV can better characterise the fault type.

4.4 Optimisation of the initial belief rule base

Due to the subjective uncertainty of expert knowledge, it is necessary to optimise the initial BRB model with a large number of training data according to the proposed optimisation algorithm in Section 3.3. The detailed steps are as follows:

Step 1 The RMSE between the one-hot encoding of the actual fault type and the output estimated results of the initial BRB is calculated as follows

$$\xi(P)=\left\{\frac{1}{600}\times\sum_{t=1}^{600}\left[Ture\_F(t)-Estimated\_F(t)\right]^2\right\}^{\wedge 0.5}.$$

Step 2 When $\xi(P)$ is the minimum value, the optimal parameter set P is found by the above objective function in step 1. The constraint conditions are $0\le\theta_k\le 1, 0\le\delta_k\le 1, 0\le\beta_{j,k}\le 1$ and $\sum_{j=1}^{6}\beta_{j,k}=1(k=1,2,...125)$. In this paper, 600 sets of sample data are used to train the BRB model by random gradient descent method. When $\xi(P) < 0.0016$, the optimal parameter set P is obtained. Partial belief rules are shown in Table 4.

Table 4 Partial rules of the optimised BRB

No	θ_k	*X1 and X2 and X3*	*Y*					
			β_1	β_2	β_3	β_4	β_5	β_6
1	0.80	VS and VS and VS	0	0	0	0	0.02	0.98
25	0.91	VS and VL and ML	0	0	0	0.18	0.82	0
50	0.55	PM and VL and VS	0	0	0.25	0.75	0	0
100	1.00	PM and PS and VL	0	0	0.55	0.45	0	0
125	0.70	VL and VL and VL	0.87	0.13	0	0	0	0

Table 5 Diagnostic results of the optimised BRB

		Fault diagnosis result							
		F6	*F5*	*F4*	*F3*	*F2*	*F1*	*Total*	*Diagnostic accuracy*
Fault type	F6	91	2	2	0	0	5	100	91%
	F5	2	95	3	0	0	0	100	95%
	F4	0	4	93	3	0	0	100	93%
	F3	0	0	2	98	0	0	100	98%
	F2	0	0	0	1	97	2	100	97%
	F1	4	0	0	3	3	90	100	90%

The fault diagnosis results of motor rotor by optimised BRB are shown in Table 5. The diagnostic accuracy of six fault types is 91%, 95%, 93%, 98%, 97% and 90% respectively, and the total fault diagnostic accuracy can reach 94%, which is significantly higher than the diagnostic accuracy before optimisation. The RMSE comparison of the fault diagnosis results of the initial BRB and the optimised BRB is shown in Figure 6. The RMSE of the optimised BRB can reach 0.2457, and the comparison shows that the optimised BRB can effectively reduce the discrete degree of fault diagnosis and improve the accuracy of diagnosis.

Figure 6 The RMSE of the initial BRB and the optimised BRB

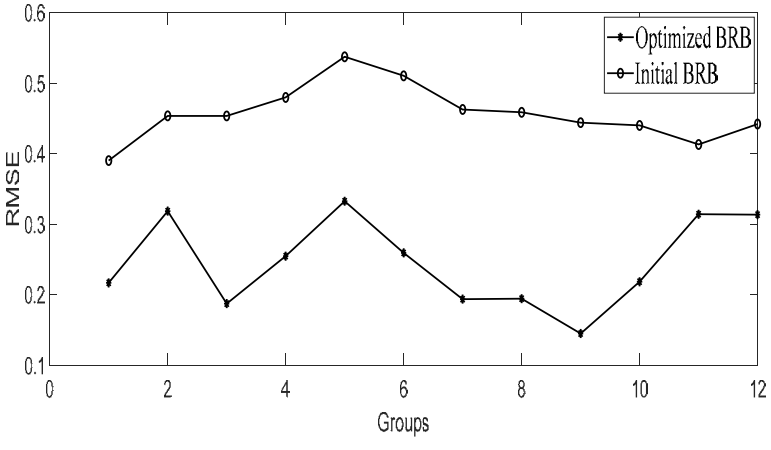

Table 6 Test diagnosis results

		Fault diagnosis result							
		F6	*F5*	*F4*	*F3*	*F2*	*F1*	*Total*	*Diagnostic accuracy*
Fault type	F6	99	2	3	0	0	6	110	90.00%
	F5	3	103	2	2	0	0	110	93.63%
	F4	0	4	101	5	0	0	110	91.82%
	F3	0	1	2	105	2	0	110	95.45%
	F2	0	0	0	4	103	3	110	93.64%
	F1	6	0	0	3	4	97	110	88.18%

4.5 Testing

In order to test the optimised BRB model, we uniformly collect 110 times data (110 × 6 = 660 sets samples) to make experiments and calculate the RMSE of diagnosis result using the proposed BRB model. Table 6 shows the confusion matrix between the real fault types of the test samples and the diagnostic fault types. The total fault diagnostic accuracy of motor rotor faults can reach 92.12%, and the RMSE of diagnosis result is 0.2841.

5 Conclusions

This paper proposes a novel rotating machinery fault diagnosis method based on data-driven and expert knowledge, which combines the fault feature extraction ability of data driven method with the uncertainty information processing ability of expert knowledge method. Then, the stability and accuracy of the model are verified and tested in experiments. The rotating machinery fault diagnosis model given in this paper has the following advantages:

1 Aiming at random spatial interference of single information source, multi-source information sensing mechanism is designed in this paper, which can effectively reduce the uncertainty of fault diagnosis results.

2 Important fault feature information is extracted by data-driven neural network algorithm, which avoids the large calculation burden and poor real-time diagnostic performance caused by using all multi-source fault information for modelling.

3 The subjective expert knowledge and objective monitoring data are fused through the belief rule-based (BRB) inference method, and the uncertain reasoning of the fusion process is carried out by using the ER algorithm. The diagnosis results cannot only judge the current fault type, but also give the probability of potential faults, which can be used to guide the inspection and maintenance of hidden faults of rotating machinery.

At the same time, it is worth noting that, there may be some problems should be studied in the future for improving the diagnosis method performance, for examples

1 This method is only an alternative method for diagnose accurately the rotating machinery fault, state estimation may be another good idea for dealing with random disturbance.

2 The influence of nonlinearity of sample size on fault diagnosis model further study.

Acknowledgements

This work was supported by the NSFC (No.62003313, 62003004, 62101507), Scientific andTechnological Research Project in Henan Province (232102241039) and Research Project of Zhengzhou Railway Vocational and Technical College(No.2022KY007).

References

Alhelou, H.H., Golshan, M.E. and Askari-Marnani, J. (2018) 'Robust sensor fault detection and isolation scheme for interconnected smart power systems in presence of RER and EVs using unknown input observer', *International Journal of Electrical Power and Energy Systems*, Vol. 99, pp.682–694, https://doi.org/10.1016/j.ijepes.2018.02.013.

Atamuradov, V., Medjaher, K. and Camci, F. (2020) 'Machine health indicator construction framework for failure diagnostics and prognostics', *Journal of Signal Processing Systems*, Vol. 92, No. 6, pp.591–609.

Bui, D., Nguyen, T. and Ngo, T. (2020) 'An artificial neural network (ANN) expert system enhanced with the electromagnetism-based firefly algorithm (EFA) for predicting the energy consumption in buildings', *Energy*, Vol. 190, No. 2020, Article ID 116370.

Chen, Y., Peng, G. and Zhu, Z. (2020) 'A novel deep learning method based on attention mechanism for bearing remaining useful life prediction', *Applied Soft Computing*, Vol. 86, No. 2020, Article ID 105919.

Cheng, C., Wang, J., Zhou, Z. and Sun, Z. (2022) 'A BRB-based effective fault diagnosis model for high-speed trains running gear systems', *IEEE Transactions on Intelligent Transportation Systems*, Vol. 23, No. 1, pp.110–121, https://doi: 10.1109/TITS.2020.3008266.

Choudhary, A., Goyal, D. and Letha, S.S. (2021) 'Infrared thermography-based fault diagnosis of induction motor bearings using machine learning', *IEEE Sens. J.*, Vol. 21, No. 2, pp.1727–1734.

Choudhary, A., Jamwal, S. and Goyal, D. (2020) 'Condition monitoring of induction motor using internet of things (IoT)', *Recent Advances in Mechanical Engineering*, No. 2020, pp.353–365.

Devarajan, G., Chinnusamy, M. and Kaliappan, L., (2021) 'Detection and classification of mechanical faults of three phase induction motor via pixels analysis of thermal image and adaptive neuro-fuzzy inference system', *J. Ambient Intell. Humaniz. Comput.*, Vol. 12, No. 2021, pp.4619–4630.

Gao, S., Zhou, Y.P. and Chen, H. (2021) 'Application of full vector-spectrum EEMD in bearing fault diagnosis', *Machinery Design and Manufacture*, Vol. 3, No. 2021, pp.118–121.

Gao, Z., Cecatl, C. and Steven, X. (2015) 'A Survey of fault diagnosis and fault -tolerant techniques', *IEEE Trasactions on Industrial Electronics*, Vol. 62, No. 6, pp.3757–3767, https://doi: 10.1109/TIE.2015.2417501.

Glowacz, A. (2021) 'Thermographic fault diagnosis of ventilation in BLDC motors', *Sensors*, Vol. 2021, No. 21, p.7245, https://doi.org/ 10.3390/s21217245.

Gonza, A., D´ıaz, I. and Cuadrado, A. (2020) 'DCNN for condition monitoring and fault detection in rotating machines and its contribution to the understanding of machine naturev', *Heliyon*, Vol. 6, No. 2.

He, M. and He, D. (2020) 'A new hybrid deep signal processing approach for bearing fault diagnosis using vibration signals', *Neurocomputing*, Vol. 396, No. 2020, pp.542–555.

Ji, S.Y., Xu, X.M. and Wen, C.L. (2017)'A kind of K-nearest neighbor fault diagnosis method based on MIV date transformation', *Chinese Automation Congress*, IEEE, pp.6306–6310.

Li, G.L., Zhou, Z.J., Hu, C.H. and Chang, L.L. (2017) 'A new safety assessment model for complex system based on the conditional generalized minimum variance and the belief rule base', *Safety Science*, Vol. 93, No. 2017, pp.108–120.

Musaw, A., Anayi, I. and Packianather, M. (2020) 'Three- phase induction motor fault detection based on thermal image segmentation', *Infrared Physics and Technology*, Vol. 104, No. 2020, p.103140.

Omar, A., Fahad, A. and Mahmoud, M. (2021) 'Sounds and acoustic emission-based early fault diagnosis of induction motor: a review study', *Advances in Mechanical Engineering*, Vol. 13, No. 2, pp.1–19.

Omar, A., Muhammad, I. and Nordin, S. (2020) 'A review of artificial intelligence methods for condition monitoring and fault diagnosis of rolling element bearings for induction motor', *Shock and Vibration*, Vol. 2020, https://doi.org/10.1155/2020/8843759.

Pham, M., Kim, J. and Kim, C.H. (2020) 'Intelligent fault diagnosis method using acoustic emission signals for bearings under complex working conditions', *Appl. Sci.*, Vol. 10, No. 20, p.7068.

Song, M.X., Sun, C.X., Cai, D.R., Hong, S.D. and Li, H.Y. (2022) 'Classifying vaguely labeled data based on evidential fusion', *Information Sciences*, Vol. 583, pp.159–173, https://doi.org/ 10.1016/j.ins2021.11.005.

Sun, G.X., Zhang, Q.H. and Shao, L.Q. (2013) 'The build of a new non-dimensional indicator for fault diagnosis in rotating machinery', *International Journal of Wireless and Mobile Computing*, Vol. 6, No. 3, pp.271–276, https://doi: 10.1504/IJWMC.2013.055770.

Wang, Z.J., Zhao, W.L. and Du, W.H. (2021) 'Data-driven fault diagnosis method based on the conversion of erosion operation signals into images and convolutional neural network', *Process Safety and Environmental Protection*, Vol. 149, pp.591–601, https://doi.org/10.1016/j.psep.2021.03.016.

Wu, C.Z., Jiang, P.C. and Ding, C. (2019) 'Intelligent fault diagnosis of rotating machinery based on one-dimensional convolutional neural network', *Computers in Industry*, Vol. 108, pp.53–61, https://doi.org/10.1016/j.compind.2018.12.001.

Wu, Z., Jiang, H. and Zhao, Z. (2020) 'An adaptive deep transfer learning method for bearing fault diagnosis', *Measurement*, Vol. 151, No. 2020, p.107227.

Wu, Z., Yang, S.P. and Liu, Y.Q. (2016) 'Rotating machinery early fault diagnosis method based on multivariate empirical mode decomposition', *Chinese Journal of Scientific Instrument*, Vol. 37, No. 2, pp.241–248.

Xu, X., Yan, X., Sheng, C. and Yuan, C. (2020) 'A belief rule-based expert system for fault diagnosis of marine diesel engines', *IEEE Transactions on Systems*, Vol. 50, No. 2, pp.656–672, https://doi: 10.1109/TSMC.2017.2759026.

Xu, X.B., Wen, C.L. and Sun, X.Y. (2017) *Evidence Fusion and Decision Method in Equipment Fault Diagnosi*, pp.1–19, Science Press, Beijing.

Yan, X., Liu, Y. and Jia, M. (2020) 'Multiscale cascading deep belief network for fault identification of rotating machinery under various working conditions', *Knowledge-Based Systems*, Vol. 193, No. 2020, p.105484.

Yu, G., Lin, T. and Wang, Z. (2020) 'Time-reassigned multi-synchro squeezing transform for bearing fault diagnosis of rotating machinery', *IEEE Transactions on Industrial Electronics*, Vol. 68, No. 2, pp.1486–1496.

Zhou, M., Liu, X.B., Yang, J.B., Chen, Y.W. and Wu, J. (2019) 'Evidential reasoning approach with multiple kinds of attributes and entropy-based weight assignment', *Knowledge-Based Systems*, Vol. 163, pp.358–375, https://doi.org/10.1016/j.knosys.2018.08.037.